Tellus (1985), *37B*, 230–242

A non-stationary model for sulphur aerosol depletion and deposition in a young spruce stand

By BO L. B. WIMAN*, *Department of Plant Ecology, University of Lund, Helgonavägen 5, S-22362 Lund, Sweden*

(Manuscript received October 23, 1984; in final form March 20, 1985)

ABSTRACT

A non-stationary partial differential equation (pde) of aerosol concentration in one space coordinate z (height above ground) is given. Submodels for the structure and aerodynamics of a young Norway spruce stand (height ~6 m) are developed from site-specific empirical data during a dry, stagnant summer period. The submodels and an empirical time series over 120 h for above-stand sulphur aerosol concentrations are used to quantify the pde and its upper boundary conditions. A simplified analysis indicates an uncertainty within one order of magnitude associated with this step. The pde-predictions of within-stand concentrations are within a factor of 2 of corresponding empirical concentration data. The associated deposition patterns show a diurnal variation and a complex z-dependency. Model improvements and further evaluation methods are suggested. The overall results suggest that estimates of aerosol deposition to forests based only on yearly and regional averages overlook strongly time and space dependent deposition patterns.

1. Introduction

The structural and aerodynamic complexity of forested landscapes should affect the aerosol dry deposition patterns in time and space (e.g. Eriksson, 1960; Hosker and Lindberg 1982; Wiman and Ågren, 1985). Such inputs include several ecologically active substances, nutrients and pollutants, affecting forest productivity (e.g. Ulrich and Pankrath, 1983). One approach to this complex problem is the development of flexible models.

In earlier work (Wiman et al., 1985) a two-dimensional *steady-state* depletion and deposition model, derived from a basic continuity equation by Wiman and Ågren (1985), has been evaluated against field data published by Wiman and Lannefors (1985). As a further step the present paper introduces a non-stationary version and empirical investigations for a model evaluation. The upper model boundary condition is defined by an empirical time series of concentrations above the stand. Model predictions and field results of sulphur aerosol concentration variations within the stand are then compared.

2. Model structure and requirements

2.1. The model

The non-stationary case in one space dimension z (height above the ground) of the continuity equation given by Wiman and Ågren (1985) reduces to

$$\partial c/\partial t = \partial/\partial z(K\,\partial c/\partial z) + v_s\,\partial c/\partial z - \rho v_d\,c + Q \quad (1)$$

where

$c(t, z, D_p)$ is aerosol mass concentration at time t of particles with diameter D_p;
$K(t, z)$ is K_{zz}-term in turbulent diffusivity tensor;
$v_s(t, z, D_p)$ is particle settling velocity;
$\rho(z)$ is vertical leaf surface area density;
$v_d(t, z, D_p)$ is deposition velocity per unit leaf area;
$Q(t, z, D_p)$ is biogeological aerosol source strength within the forest.

* Present affiliation: Environmental Studies Programme, University of Lund, Gerdagatan 13, S-22362 Lund, Sweden.

This formulation requires that: (i) terms other than K_{zz} in the diffusivity tensor can be neglected; this is a common practice for the current type of problem (e.g. Dobbins, 1979) and seems well founded (cf. Yeh and Brutsaert, 1971). Further, unless the stand is extremely heterogenous, the horizontal wind components, not K_{xx} and K_{yy}, should be responsible for horizontal mass transfer. In this paper I follow the convention (though debatable; e.g. Munn, 1966; Hosker and Lindberg, 1982) of neglecting differences between momentum and mass transfer; (ii) the wind velocity field is divergence-free; unless abnormal situations are at hand (such as extreme edge effects) this holds (cf. Businger, 1982; Wiman and Agren, 1985); (iii) gradients of wind speed and concentration in the x- and y-directions can be neglected, implying that local equilibrium with respect to x and y can be assumed. This should be the case for a reasonably homogenous stand (or section of it) a couple of stand heights away from distinct forest walls (cf. Wiman and Agren, 1985). Numerical methods for handling eq. (1), including the one used here normally require that for efficient use the functions defining the partial differential equation (pde) should be 'smooth' (continuous 1st derivatives). Thus, rather than directly using field data for input to eq. (1) they should be processed to smooth submodels. Problems involved in numerical handling of pde:s are further discussed by, e.g. Dobbins (1979).

2.2. *Subfunctions for aerodynamics*

To link above-canopy processes with sub-canopy ones, define the upper canopy limit at $z = z_c$ and the upper model boundary at $z = z_r$. In this paper, $z_r = 1.3z_c$. With

$$K(t, z) = l_m(z)^2 \, \partial u(t, z)/\partial z S(t, z) \qquad (2)$$

field information is needed for the mixing length l_m, effective value of horizontal wind speed u and stability function S. Following Perrier (1976) gives

$$l_m = kL(z) \qquad z \le z_c$$

$$l_m = k(z - z_c) + kL(z_c) \quad z \ge z_c \qquad (3)$$

where k is von Karman's constant and $L(z)$ is approximately related to stand structure through $L(z) = (1 - \exp(-\mathrm{LAI}_{st}/(z_c/w)z))/(\mathrm{LAI}_{st}/(z_c/w))$. Here LAI_{st} is the large scale leaf area index (two-sided) of the stand and w a factor accounting for the orientation of the leaves (needles) (cf. the Appendix).

Connecting a sub-canopy hyperbolic wind profile model (Cowan, 1968) with an above-canopy logarithmic one gives, with $u_c = u(t, z_c)$

$$u(t, z) = u_c \, (\sinh(Az \cdot z_c^{-1})/\sinh(A))^{0.5} \qquad z \le z_c$$

$$u(t, z) = u_c/\ln((z_c - d)/z_0) \ln((z - d)/z_0) \qquad z \ge z_c \qquad (4)$$

where A is determined by demanding that $\partial u/\partial z$ be continuous at $z = z_c$, giving: $A = ((2z_c)/(z_c - d))/\ln((z_c - d)/z_0)$. The zero plane displacement (d) is given by $d = (1 - L(z)/z_c)z_c$ (Perrier, 1976) and the roughness length (z_0) from the average size of eddies at the canopy top (e.g. Monteith, 1973), $z_0 = k(z_c - d) = kL(z_c)$.

The function (S) describing stability/instability within and above the stand is a function of Richardson's number, Ri. The relationships given by Goudriaan (1977) (working with S^{-1} and slightly redefining Ri for sub-canopy use) are used in the present study. See also Thom (1975). Ri is defined from l_m, u, the gravitational constant, absolute air temperature and the equivalent temperature, in turn a well defined function of air temperature (T_a), relative humidity (rh), water vapour saturation pressure and height z. The region $\mathrm{Ri} \ge 0.1$ is experimentally and mathematically troublesome as S tends rapidly towards 0; the expression for S collapses for $\mathrm{Ri} \ge 1/4.7$. To avoid unnecessary sensitivity to field data imperfections and unrealistic situations tending towards extreme stability, the restriction $\mathrm{Ri} \le 0.1$ is used in the present study. Thus, eq. (2) is defined from micrometeorological and structural data obtainable from field measurements.

2.3. *Subfunctions for aerosol mechanics and foliage distribution*

v_s and v_d can be assigned formulations based on aerosol physics in combination with experimental (such as wind tunnel) data. Wiman and Ågren (1985) used an expression (based on filtration theory) where terms accounting for diffusion (indicated by suffix 'diff' below), impaction ('imp') and gravitational settling (v_s), respectively, were linearly added:

$$v_d = u a\mathrm{diff} \, \mathrm{Pe}^{-b\mathrm{diff}} + u(\mathrm{St}/(\mathrm{St} + a\mathrm{imp}))^{b\mathrm{imp}} + v_s w \qquad (5)$$

where Pe is the Peclet number; St is the Stokes number. For consistency, *a*diff, *b*diff, *a*imp and *b*imp are assigned the same values here as in the stationary model evaluation by Wiman et al. (1985) for a mature coniferous forest: 3, 0.5, 3 and 1, respectively. Site specificity is entered into eq. (5) through the characteristic dimension d_n, the mean diameter of spruce needles at the site (cf. the Appendix). The determination of $\rho(z)$ from site measurements is treated in detail in the Appendix.

2.4. *Initial and boundary conditions*

If the sampling points of concentration are insufficient to determine initial conditions ($c(t = 0, z) = c_0$) initializing is best made from a steady state solution of eq. (1). This procedure also informs about the time constants involved and suggests relevant time steps. The boundary condition for $t \geq 0$, $z = z_r$, can be defined by the measured above-canopy concentration data with linear interpolation between data points. The determination of the associated particle size distribution can be based on empirical data and/or accepted generalizations (such as log-normal models). For $t \geq 0$, $z = z_s$ (lower canopy limit) $\partial c/\partial z = 0$ is a good choice for such canopies where z_0 tends towards zero (cf. also Wiman and Ågren, 1985).

3. Experimental

3.1. *The field site*

The experimental site (Fig. 1) is within a larger array of sampling sites in the southern border zone of the boreo-nemoral region of Sweden (the Boalt study area, 56°20′N 13°30′E; cf. Wiman and Lannefors, (1985); for consistency the present site is named 'station no. 5'). The site consists of 1 hectare of Norway spruce planted in 1971–72. At the time of the study (August 1982) tree heights were around 6 m (= z_c) and the canopy cover around 50%. These and other properties were estimated to correspond to a large scale leaf (needle) area index (LAI_{st}, two-sided) of 10 and a stand specific vertical distribution of needle surface area in unit forest volume (ρ_{st}) described by a chi-square type of expression (cf. the Appendix). A floristic and forestry inventory showed an intermediate successional stage of the stand, remains from the clear-cut phase (such as *Rubus idaeus* (L.)) being rare. Sampling of aerosol and micrometeorological data were carried out from

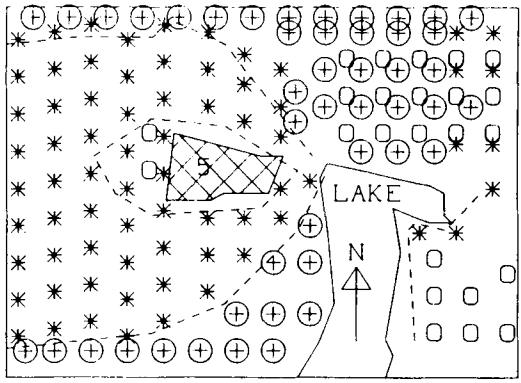

Fig. 1. The experimental site (cross-hatched, sampling station at '5') and surroundings. (*) Norway spruce, tree heights ~20 m. (⊕) Scots pine, 10–15 m, (○) birch (occasionally beech), 10–15 m. Dashed lines indicate elevation contours (c. 5 m change between contours).

August 1st, 20.00 to August 6th, 20.00 (local time is GT + 1 h). Surface weather maps show this period to be dry, warm and stable over southern Scandinavia.

3.2. *Aerosol sampling and analysis*

The aerosol was characterized with three independent methods: particle number concentration sampling in 7 size classes with a Climet 208C optical particle counter (OPC) (e.g. Husar, 1974), mass concentration sampling with a two-stage filter equipment (cf. Cahill et al., 1979) and cascade impactor sampling (Batelle single orifice type). Combining these methods gives certain possibilities to estimate the size distribution of the sulphur aerosol (cf. section 4.1).

OPC-data from 7 classes (0.3–0.5, 0.5–0.7, 0.7–1, 1–3, 3–5, 5–7 and 7–10 μm) were obtained above (at height 7.5 m) and within (at 1 m) the stand through sequential sampling over the 7 classes (1 min. integration time, flow rate 7.1 l min^{-1}). The sequence was repeated above/within the stand through an electronically triggered switching system, implying a time lag of 10 min. between sampling of a given class above/within the stand. The particle sensor was positioned halfway between the two sampling points implying tube lengths of 3.5 m from each inlet to the OPC. The switching system consisted of a Y-formed tube section connected to two magnetic valves with smooth transmission paths. The inlets were of funnel type with inlet dia. 50 mm. Laboratory and

field tests showed no detectable bias with respect to the two 'tube channels'. The sampling efficiencies of the tube-valve system relative to the efficiency without tube and valves were, for the 7 classes respectively (±one standard deviation): 1.0 (0.001), 1.0 (0.004), 1.0 (0.007), 0.9 (0.01), 0.9 (0.1), 0.8 (0.3), 0.6 (0.4).

Aerosol mass concentrations, for later analysis with particle induced X-ray emission analysis (PIXE) (Malmqvist et al., 1982), were sampled at the heights 7.5 and 1 m during each 12-h block of the period (thus 'night', 'day', etc.) by means of an inlet – filter – tube assembly (flow rate 1.1–1.5 l min.$^{-1}$). The inlets were of nozzle type with inlet diameters 2.0 (4.0) above (within) the stand. This strategy for low-volume sampling should reduce the sampling bias due to the different aerodynamic conditions above/within the canopy to the range <5% and 10–20% for fine (aerodynamic dia. <c. 2 μm) and coarse particles (up to c. 7 μm), respectively (Wiman and Lannefors, 1985). The filter assembly consisted of a pre-stage for coarse particle sampling (25 mm dia. Nuclepore filter, 8.0 μm pore size, apiezon coated) and 2nd stage (13 mm dia. Nuclepore, 0.4 μm pore size); cf. Spurny and Lodge (1972), Liu et al. (1983).

Two above-canopy cascade impactor samples were also retrieved (2 × 12 h sampling, flow rate 1 l min.$^{-1}$, inlets as those for filter sampling attached). After exposure filters and impactor plates were analysed for sulphur at the PIXE set-up, Dept. of Nuclear Physics, University of Lund, Sweden.

3.3. *Sampling of micrometeorological data*

Temperature was sampled every 30 minutes throughout the period, at 8 levels (7.5, 5.5, 4.7, 3.9, 3.0, 2.3, 1.5 and 0 m) by means of thermistors connected to a timer-recorder. Wind speed was continuously recorded by cup anemometers at the levels 7.5, 6.2, 3.7 and 0.5 m. Relative humidity was continuously recorded with hygrographs at the levels 5.1, 1.3 and 0.3 m.

3.4. *Data handling*

OPC-data for each class were added for each 12-h block. The representativity error of the resulting data is the major one and is essentially related to the sampling restriction (1 min each 20th min). Independent tests with continuous 1 min

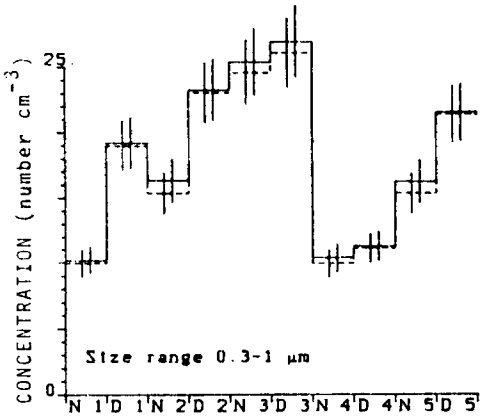

Fig. 2. Number concentrations within the OPC-range 0.30–1 μm. N1, D1 etc refer to 'night no. 1', 'day no. 1' etc. Errors due to the time lag between measurements indicated.

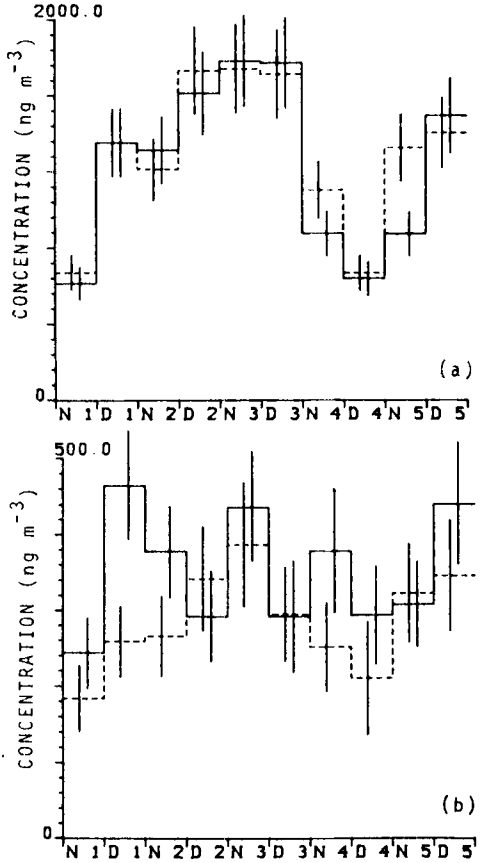

Fig. 3. Fine (a) and coarse (b) sulphur concentration variations during the period. Solid (dashed) line: above (within) the stand. Error bars correspond to one standard deviation.

sampling showed the concentrations of fine particles normally to change less than 10% over 20 min.; changes in coarse particle concentrations were in the range 50% over 20 min. (1–3 μm class) up to a factor of 10 (3–10 μm classes). This suggests that the 12-h block data for the range 0.3–1 μm (Fig. 2) offer meaningful comparisons with sulphur aerosol concentrations. For coarse particles knowledge of underlying processes (such as (re)suspension of needle particles and fragments), particle refractive index and detailed statistical models—beyond the scope here—are needed to adequately estimate representativity errors; thus coarse particle data are not further used in the present study.

Mass concentration data for fine and coarse sulphur fractions were treated with respect to error calculations according to Wiman and Lannefors (1985). Overall errors (corresponding to one standard deviation) for fine (coarse) sulphur concentrations were generally <15 (25)%, including sampling bias. Results are shown in Fig. 3. Impactor data were treated analogously, then time averaged to cover 24 hours, cf. Fig. 4. Considering the interstage loss problem of impactors (e.g. Marple and Willeke, 1976) the resulting distribution might be somewhat shifted towards smaller particles relative to the true distribution. Also, fully representative low-volume sampling of particles $\gtrsim 8$ μm is practically unattainable in most field situations and mass concentrations of particles above this value are probably underestimated.

Temperature, wind speed and relative humidity data for corresponding sampling occasions during the five 24-h blocks were averaged between days. Due to the stable large scale weather the diurnal cycles in the stand were similar over the period and

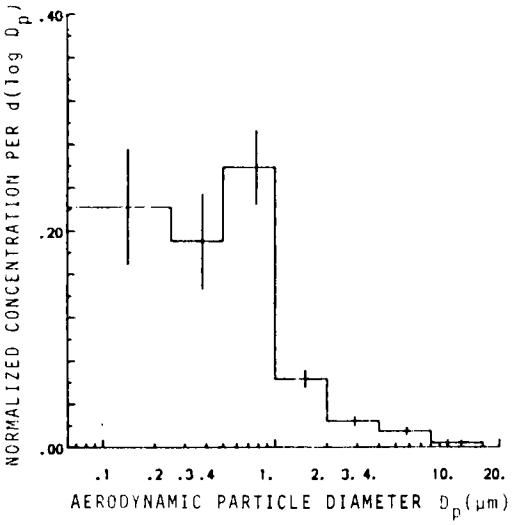

Fig. 4. Time averaged particle size distribution (normalized) of the sulphur aerosol over 24 h. Left and right limits used to present fractions obtained on the 7th and 1st impactor stages. The column areas give the relative mass loads on each stage. Error bars as in Fig. 3.

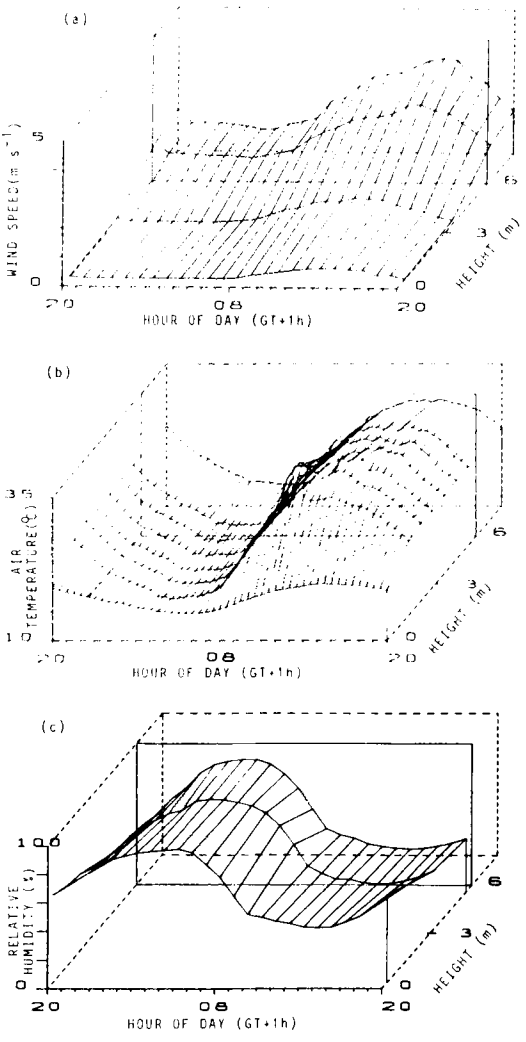

Fig. 5. Field data (averaged between 5 days) over 24 hours for (a) wind speed u, (b) air temperature T_a and (c) relative humidity rh at the sampling station as a function of time t and height z above ground. Upper canopy limit indicated by solid-lined rectangle. For input to the pde-model curve and surface fitting are employed.

the resulting mean diurnal lapse for these variables is well representative (coefficients of variation are less than 15 %). Results are shown in Fig. 5.

4. Submodels

4.1. Aerodynamics

From the analysis in section 2, in combination with the sinusoidal character of the micrometeorological data, the following expressions were obtained through curve and surface fitting (t in hours). Differences between the empirical mean diurnal lapse and the fitted surfaces are typically less than 10%, occasionally 30% where the sine-function simplification creates the main distortion. Major empirical characteristics are, however, maintained.

Wind speed. $u(t, z)$ as detailed in section 2, with the quantifying parameters A, d and z_0 calculated from $\mathrm{LAI}_{st} = 10$, $z_c = 6$ (cf. the Appendix) and $u_c(t) = 0.75 \sin(\pi t/12 + \pi) + 1.25$.

Air temperature. $T_a(t, z) = p(z) \sin(\pi t/12) + q(z)$ where $p(z) = 8.5 - 0.00023\ (\mathrm{abs}(z - 4.5))^{6.76}$; $q(z) = 22.4 - 0.01\ (\mathrm{abs}(z - 4.5))^{4.13}$.

Relative humidity. $rh(t, z) = (23.5 \sin(\pi t/12) + 65.1) \exp(-0.040z)$.

For water vapour saturation pressure, needed to complete the calculation of the equivalent temperature, a close and smooth fit was constructed from tabulated data.

Stability and eddy diffusivity can then be calculated. Technically, all submodels are incorporated and further handled (with respect to derivatives etc.) in the final Fortran program solving eq. (1). The resulting K-function is shown in Fig. 6.

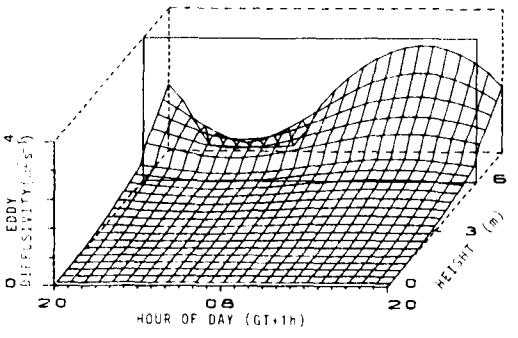

Fig. 6. Submodel $K(t, z)$ (eddy diffusivity function) resulting from the submodels for stand structure and micrometeorology. The K-surface bends downwards above the canopy during night.

4.2. Concentrations and particle size distributions at the upper boundary

Comparing Figs. 2 and 3a suggest that fine particle OPC-data were good tracers of fine fraction sulphur concentrations. Correlation analysis of the concomitant variation between these independent observations yielded $r = 0.96$ and 0.64 with respect to the 0.3–0.5 and 0.5–0.7 μm OPC classes, respectively. Remaining combinations gave insignificant correlations. For coarse sulphur the corresponding investigation cannot be conclusively interpreted (cf. 3.4). This first step, however, indicates that particles below 0.7 μm (optical dia.) are major contributors to fine sulphur fractions as recorded on the 2nd stage filter. Assuming particle densities up to 2 g cm^{-3}, the value corresponds to around 1 μm aerodynamic dia.

The general feature of the impactor-sampled distribution of sulphur (Fig. 4)—a dominating sub-μm particle fraction and a small but significant super-μm fraction—compares well with impactor samples of sulphate investigated by Whitby (1978) and is consistent with the OPC-information. From Fig. 4 only, there can be no certain conclusion whether super-μm fractions are merely a 'tail' from the accumulation mode or whether they indicate the existence of an independent coarse sulphur mode. However, particles of several μm 'tailing' from accumulation mode are not likely, considering the source mechanisms in action (Whitby, 1978). Correlation analysis shows a fairly low degree of association between fine and coarse sulphur fractions ($r = 0.44$). This suggests that during the period, sulphur is best understood as occurring in two modes with intermingling tails, one dominating accumulation mode (anthropogenically influenced) and one coarse mode (associated with the maritime influence at the site, possibly also with windblown organic fragments).

Including the operational mode of the filter system (implying that some particles smaller (larger) than the 50% cut off dia. of 2 μm will be captured by (penetrate to) the 1st (2nd) filter stage) the available information can be consistently summed up to a best practical approach where the sulphur aerosol distribution is modelled as one digitized lognormal mode with aerodynamic geo-

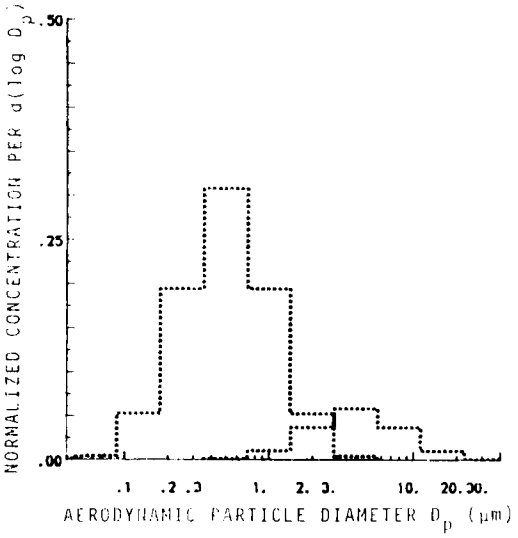

Fig. 7. Generalized particle size distribution model of sulphur used for input to eq. (1). The column areas give the relative mass loads of each interval. When used in eq. (1) the ratio between the concentrations of the two modes is varied according to empirical ratios between fine and coarse fractions. The mean ratio 4:1 is used in this diagram.

metric mean dia. (D_{pg}) 0.5 μm and geometric standard deviation (σ_g) 2, followed by a coarse mode with D_{pg} = 4 μm, σ_g = 2. Cf. Fig. 7. The resulting overall model distribution compares well with background sulphur aerosol distributions of southern Sweden given by Lannefors et al. (1983).

As the relative contributions of the respective sulphur modes in Fig. 7 change with time a resulting time-variant overall model distribution obtains. Technically, the empirically found relative contributions for each 12-h block were entered into the pde-algorithm which then first operated on each of the 7 particle classes of the fine-particle oriented mode, then on the 7 coarse classes. Thus analysis of model performance with respect to concentrations of each mode as well as total concentrations was carried out.

5. A simplified sensitivity analysis

This study has two main phases. (1) Field data are obtained and processed to submodels. These submodels are used to quantify eq. (1). (2) The performance of the pde is investigated relative to empirical concentration data independent of phase (1). Given the field data were completely error-free and submodels were *a priori* corroborated, phase (2) would unambiguously test the validity of the pde-*structure*. This situation is not at hand and the outcome of phase (2) must be interpreted with respect to the uncertainty embedded in phase (1). Major sources of uncertainty in the 1st phase are: (i) field data imperfections, (ii) curve and surface fitting imperfections, (iii) imperfect formulations of K, v_d and the particle size distribution. Sources (i) and (ii) introduce local uncertainty up to around 50%; LAI_{st} is a dominating source. The formulation of v_d was constructed by Wiman and Ågren (1985) from filtration theory and matched with experimental data by Little and Wiffen (1977); it should be within the correct order of magnitude. The critical parameters of the particle size distribution are the geometric mean diameters, likely to be safe within a factor of 2. I judge the formulation of the K-function to introduce the major uncertainty in phase (1), as it may also introduce a *qualitative* deficiency into eq. (1), notably for non-neutral situations.

A detailed assessment of the overall uncertainty introduced by these sources into eq. (1) is a complex task. However, neglecting possible functional deficiencies inherent in K a simplified analysis can be employed through investigating the stationary case of eq. (1) and setting ρ, v_d and K constants, thus yielding a manageable ordinary 2nd order differential equation in concentration c. Investigations of the sensitivity of the differential dc to changes in other differentials, notably $d\varepsilon$, where $\varepsilon = \sqrt{\rho v_d/K}$, showed that $|dc/c|$ is around 0.5 for $|d\varepsilon/\varepsilon|$ around 10 with sensitivity increasing with decreasing z. Although simplified, the analysis indicates (probably conservatively) that phase (1) of the present study has quantified eq. (1) within the correct order of magnitude. As the smoothening-procedure enables algorithmic local numerical error-control at the 5%-level, pde-results within one order of magnitude relative to data available for comparison should be expected if the pde-structure is to demonstrate any capacity of reproducing the field situation.

6. Results and discussion

6.1. The submodels

The Appendix shows that a chi-square type of distribution for vertical leaf area density well

approximates the stand conditions, representative of an intermediate successional stage of stands managed with common forestry methods. The hyperbolic-logarithmic wind profile formulation based on site specific structural data compares well with the independently obtained wind data. This suggests a potential for operational use of the wind submodel. The lack of biophysically founded and high-precision submodels of temperature and relative humidity is, however, a clear drawback of this study. The approach chosen here is surface fitting; for situations where the sine-function simplification is obviously impracticable (strong frontal activity) refined techniques are necessary unless simplified by *a priori*-knowledge about the underlying type of fitting function. Although the net result of the submodels comes out as an eddy diffusivity function performing well when compared with experience from other crops, this cannot be used to invoke independent confidence in the pde-model results (cf. section 5).

6.2. *Pde-model results versus empirical concentrations*

Running the model for the conditions detailed above (where a time step around 15 min. was found numerically appropriate) yields the results shown in Fig. 8, where measured concentration data are incorporated for comparison. The model predictions of the concentration variations within the stand are satisfactory from to essential aspects: (a) predictions for total, fine and coarse sulphur concentrations are clearly of the correct order of magnitude; (b) the correct type of rapid response to the changing boundary conditions is obtained.

Further, several empirical situations indicating concentration depletion are predicted by the model. This point was further investigated by comparing the 12-h averaged predictions for the coarse/total ratios within the stand with those obtained empirically. The field data shows that the larger this ratio above the stand, the larger is the difference between the ratios above and within the canopy. This shows that depletion is more (less) effective the more the aerosol assumes a coarse-particle (fine-particle) oriented distribution and thus emphasizes the distinction between transfer and deposition of fine particles (negligible gravitational settling, eddy transfer dominant, inefficient diffusional deposition) and coarse particles (gravitational settling and eddy transfer, effective deposition

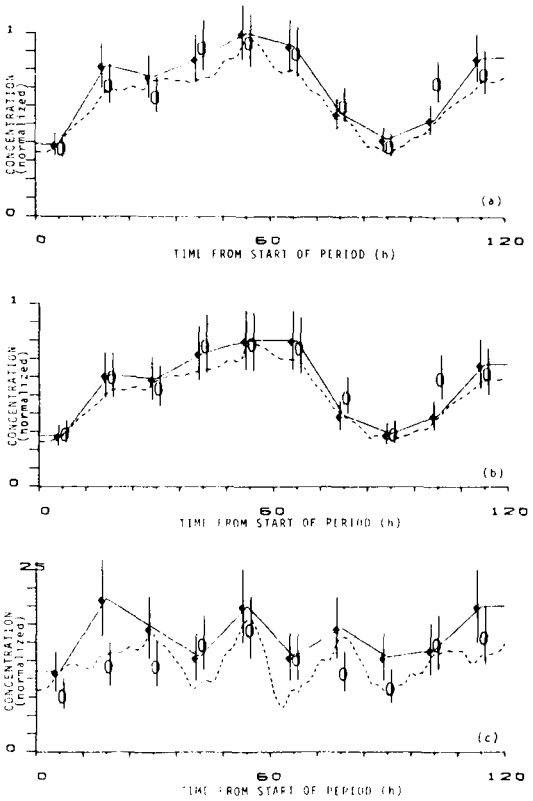

Fig. 8. Pde-model result for sulphur aerosol concentration $c(t, z)$ above (z = 7.5 m, solid line) and within (z = 1, dashed line) the stand. Field data above (*) and within (0) the stand are given; error bars correspond to one standard deviation. (a) is total, (b) fine and (c) coarse concentrations. Model results are given with a resolution of 1 h. Maximum total concentration is normalized to 1.

due to impaction and sedimentation). This empirical result, consistent with independent findings by Gravenhorst and Höfken (1982); cf. also Wiman and Lannefors (1985); Wiman *et al.* (1985), is qualitatively predicted by the model (correlation between predicted and empirical ratios within the stand is 0.80).

However, it is also clear that the model fails to predict the detailed behaviour of field concentration data. Discrepancies in terms of predicted relative to empirical concentrations are in the range 0.67–1.07 for fine concentrations and 0.66–1.5 for coarse concentrations, with means 0.91 and 1.06, respectively. This can be compared with the error boundaries implied in the empirical data, ±15% (25%) for fine (coarse) concentrations. Using

quadratic addition of errors for the measured concentration differences, there are 2–3 empirical cases with statistically significant depletion of the coarse concentrations. 9 (7) cases involve insignificant depletion of fine (coarse) concentrations; in one case significant enrichment (reversed concentration gradient) of fine particles occurs. The failure of the model to predict enrichment suggest a qualitative deficiency attributed to incomplete description of (fine) particle transfer.

Accepting the worst case (i.e. including empirical errors in sub-canopy concentration data) as a measure of model performance, model predictions of sub-canopy concentrations are within a factor of 2. This should be acceptable from the aspect that the model is clearly capable of a meaningful handling of a non-trivial composition of counteracting forces. It is unsatisfactory from the aspect of operational use of the model, as it is, at present, difficult to assess stringently how the uncertainty introduced with the submodels propagate through the process. It is also clear, that a much refined high-precision data base for concentrations and particle size distributions (including effects of relative humidity on hygroscopic particles) is needed for further model evaluation.

The overall result justifies an investigation of the full solution of eq. (1) with respect to concentration (Fig. 9) and deposition (Fig. 10). The vertical concentration gradient is predicted as negligible for fine (Fig. 9a) and coarse (Fig. 9b) particles in the upper half of the canopy; here concentration depletion is balanced by turbulent inputs and, for coarse particles, inputs due to gravitationally settling particles. Within the lower half of the canopy leaf surface area density increases, thus presenting a large number of particle collectors. However, the increased needle density also leads to decreasing wind speed (and decreased deposition velocities) and ineffective turbulent transfer, particularly during stable daytime conditions. For this part of the canopy, the model predicts significant depletion as a net result of the counteracting forces.

The patterns of the deposition rate per unit ground area (r_g) for fine (Fig. 10a) and coarse (Fig. 10b) particles add further information. The most pronounced effects are (i) the distinct qualitative and quantitative difference between fine and coarse particle deposition, (ii) the increase of deposition rates during daytime. The interplay between above-stand concentrations, aerodynamics and structure

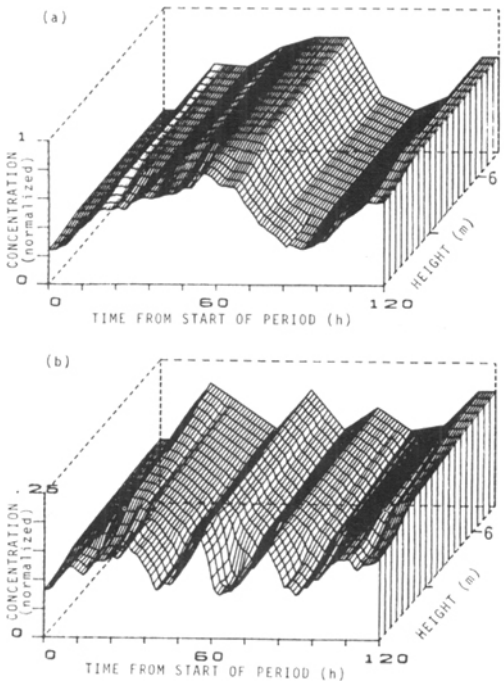

Fig. 9. Full pde-solution for sulphur aerosol concentration $c(t, z)$ at the site. (a) fine, (b) coarse concentrations. Normalization is such that the value 1 represents maximum total concentration.

results in only a weak z-dependency for fine particle deposition over the upper half of the canopy; further down where transfer, wind speed and needle density decline, deposition also decreases. For coarse particles, deposition seems to decrease approximately as a linear function of the downward distance from canopy top. Maximum coarse particle deposition takes a value a factor of 5 above maximum fine particle deposition values (despite the fact that above-canopy coarse concentrations are a factor of 3 lower than fine concentrations).

Quantifying and integrating the deposition patterns of Fig. 10 give the values of 6 (7) mg m^{-2} as the model estimates of fine (coarse) sulphur deposition rates *over the 120-h period.* In terms of gross canopy deposition velocity these rates correspond to 1 and 4.5 cm s^{-1}, respectively, when evaluated from mean concentrations over the period (cf. Fig. 3). Hicks (1980), summing up on the fine particle deposition problem, concludes that the possible range should be 0.1 cm s^{-1} (conventional viewpoint) to 1 cm s^{-1} (highest likely long-

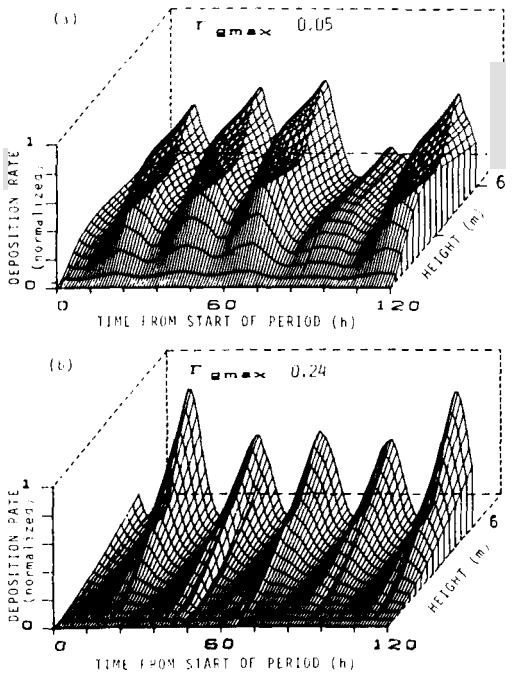

Fig. 10. Full pde-solution for sulphur aerosol deposition rates r_g (t, z) at the site. (a) fine, (b) coarse fractions. Normalization is such that the value 1 represents maximum fine fraction deposition in (a) and maximum coarse fraction deposition in (b). Comparison is obtained through the respective relative maximum value $r_{g\max}$ given in each figure. Lines 'behind the ridges' are not hidden.

term value over any continental natural surface), with 0.4 cm s^{-1} as a most likely average value. The fine fraction values can also be compared with the estimate of 0.3 mg m^{-2} day (0.4 cm s^{-1}) given by Wiman (1981) generalizing from wind tunnel data to a pine forest with leaf area index around 5 and exposed to a sulphur aerosol of 1000 ng m^{-3}. This is supportive of a good potential for further model improvements. As the pde-model is broken down into submodels systematic refinement procedures are possible. Overcoming deficiencies with respect to the formulation of the K-function is likely to be the most important (and complex) step towards an operational model. In particular, turbulence effects not accounted for by the stand homogeneity assumption must be incorporated. Further, the momentum-mass similarity approach, though a common first-order approximation, is likely to overlook particle transfer processes leading to reversed concentration gradients.

7. Conclusions

Measured in-canopy concentrations of *fine-particle* sulphur differed insignificantly from above-stand concentrations. On the average, in-canopy concentrations predicted by the pde-model were 90% of empirical values; thus the model overestimated particle deposition and/or underestimated turbulent transfer. Empirical in-canopy *coarse-particle* concentrations were below above-canopy concentrations in most 12-h sampling blocks; significant depletion down to 54% of above-canopy concentrations was observed. On the average, in-canopy concentrations predicted by the model were 106% of empirical values; thus particle deposition was underestimated and/or downward particle flux was overestimated. Considering errors in empirical concentration test data, model predictions of within-canopy concentrations may be in error up to a factor of 2. Model predictions of gross canopy fine particle deposition are around the upper limit (1 cm s^{-1}) suggested by independent experimental data. Qualitatively, the model predicts diurnal and spatial distinctions in the deposition patterns of fine and coarse sulphur aerosols. Such distinctions are overlooked by standard methods for long-term and large-scale deposition estimates.

Further quantitative refinement of the model is necessary to assess its operationality; the submodel structure faciliates such procedures. The momentum-mass similarity used in this study may well be incomplete for the description of particle transfer, especially in unstable conditions.

8. Acknowledgements

This work was carried out with financial support from the National Swedish Environment Protection Board and from the Swedish Natural Science Research Council. I thank G. I. Ågren for constructive discussions on the modelling parts and H. O. Lannefors for PIXE-work, field assistance and helpful criticism. The theme of this paper would not have been developed without the contributions of these colleagues to earlier work published elsewhere. I also thank B. Nihlgård and H. Staaf for helpful comments on the stand structural analysis; K. Malmqvist, H.-C. Hansson and other PIXE-people for supportive discussions; G. Hansson for laboratory assistance; A.-K.

Ekholm for PIXE-spectra fits; L. B. Nilsson for help with field constructions; G. Cöster for access to the field site. I also thank three unknown reviewers for constructive criticism of an earlier version of this paper.

9. Appendix. A vertical foliage distribution and leaf area index (two-sided)

Studies by Swank and Schreuder (1974), Ross (1975), Ford (1976), Holmes and McCartney (1976), Monteith (1976), Massman (1982), Wiman et al. (1985) exemplify various methods for determining foliage distributions with indirect (such as based on light or coarse particle penetration) and direct measurements. A direct method with four main steps is used in the present study.

(1) *Determination of needle surface area to dry mass ratio, S_m*

Ten needles at the tree height c. 1 m and ten at c. 4 m were sampled from each of five spruce trees at the site. The maximum (d_1) and minimum (d_2) diameters at the middle of each needle were determined as was the length (l) of each needle. The dry weight of each sample of ten needles was then determined. The needle surface area is represented by the formula $2l\sqrt{(d_1^2 + d_2^2)}$ (rhomboid with negligible end surface area). Using all ten samples yielded S_m (± one standard deviation) = 14(3) m^2 kg^{-1}. This can be compared with Massman (1982) giving 13.5 m^2 kg^{-1} for Douglas fir and sugar pine in Oregon. The mean needle diameter (d_n) used as characteristic dimension in model applications (cf. Section 2.3) was also obtained as the mean of 0.5 ($d_1 + d_2$) for the ten samples; $d_n = 0.8$ (±0.2) mm.

(2) *Characterization of a spruce tree*

One spruce tree, 5.7 m high (11 years old) was sampled at the site and cut into 11 strata (each stratum corresponding to its age). The height h_i of each stratum was measured and also l_i, its average branch extension (apparent length from the stem centre). The needle dry weight W_i of each stratum was determined. The needle surface area density D_i of each stratum was then calculated as $D_i = W_i (S_m (A_p h_i)^{-1})$, where A_p is the projected ground surface area of the tree; $A_p = \pi l_{max}^2$ where l_{max} is maximum l_i value obtained. The leaf area index

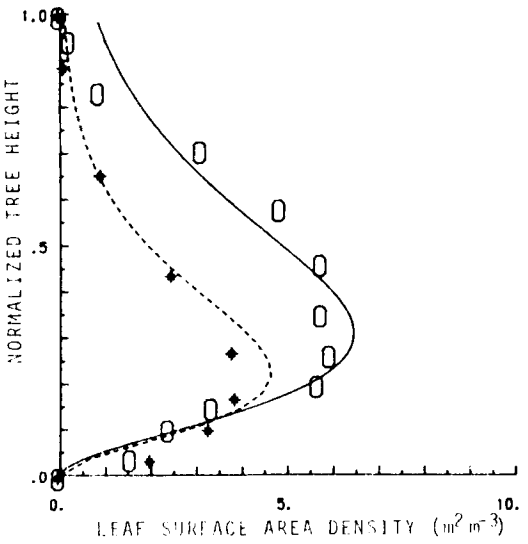

Fig. A1. Field data for leaf (needle) surface area density as a function of normalized height z_n; (O) and (*): Norway spruce tree, age 7 and 11 years, respectively. Leaf area density submodel ρ as a function of z_n; dashed line (solid line): age 7 (11) years.

under the tree (LAI_t) was calculated as

$$LAI_t = \left(\sum_{i=1}^{j} W_i S_m \right) A_p^{-1}$$

(j is total number of strata), yielding LAI_t = 20 m^2 m^{-2}. For comparison the same procedure was carried out with a 2.8 m high tree (7 years old), giving LAI = 5.3 m^2 m^{-2}. The D_i-values are plotted vs the normalized tree height $z_n = (z - z_g)/(z_c - z_g)$ in Fig. A1 (z is height above ground, z_g is lower canopy limit = 0 m for both trees, z_c is tree height).

(3) *A function for needle surface area density, $\rho(z)$*

The following form was found useful: $\rho(z) = LAI_t(z_c) z_n^2 \exp(-az_n)$ where $LAI_t(z_c)$ is leaf area index under a tree with height z_c, a is a shape factor and normalizing is obtained by

$$\alpha = \int_{z_g}^{z_c} z_n^2 \exp(-\alpha z_n)/\alpha_n dz.$$

A good fit to the field data was obtained with a = 6.5 and 9 for the 11 and 7 years old tree, respectively (cf. Fig. A1).

(4) *Generalization to the stand*

An estimate of the large scale index LAI_{st} (hectare per hectare of ground area) is obtained

through $LAI_{st} = PLAI_t$ where P is the canopy cover, estimated to 50% based on the average spacing between trees and average extension of the crowns. An estimate of the error in LAI_{st} can be made from $LAI_{st} = PS_m W_{tot} (\pi l_{max}^2)^{-1}$, where W_{tot} is total dry needle weight of a tree. Differentiation and quadratic addition of errors give $dLAI_{st} = \pm 4$ hectare hectare^{-1} with the following partial errors: $dP/P = 25\%$, $dS_m/S_m = 25\%$, $dW_{tot}/W_{tot} = 10\%$, $dl_{max}/l_{max} = 10\%$. The shape properties of $\rho(z)$ are unlikely to differ much between trees. Thus, the vertical needle surface area density large scale distribution ρ used in this study is

$$\rho(z) = 10 z_n^2 \exp(-6.5 z_n)/a_n \quad \text{with } \rho = 0, \quad z > z_c.$$

When used in connection with the present formulation of eq. (5) total needle surface area (both sides) operates on the diffusion and impaction terms. For the settling term needle shapes and orientations (incorporated in the factor w must be considered. Detailed determinations are unnecessarily complicated for the present scope; the shape model together with orientations distributed between fully random and fully horizontal leads to an estimate of $w = 0.25$ for use in this study.

The temporal aspects of this problem during stand succession are indicated by the comparison with the 7 years old tree and the estimates for a mature forest based on other procedures in Wiman et al. (1985); cf. also Jarvis et al. (1976), Rauner (1976).

REFERENCES

Businger, J. A. 1982. Equations and concepts. In *Atmospheric turbulence and air pollution modelling* (ed. F. T. M. Nieuwstadt and H. van Dop). Reidel, Dordrecht, 1–36.

Cahill, T. A., Eldred, R. A., Barone, J. and Ashbaugh, L. 1979. Ambient aerosol sampling with stacked filter units. Report No. FHWA-RD-78-178. Federal Highway Administration, Offices of Research and Development, Washington D.C., 20590, U.S.A.

Cowan, I. R. 1968. Mass, heat and momentum exchange between stands of plants and their environment. *Q. J. R. Meteorol Soc. 94*, 318–332.

Dobbins, R. A. 1979. *Atmospheric motion and air pollution modelling.* Wiley and Sons, Toronto, 250–282.

Eriksson, E. 1960. The yearly circulation of chloride and sulphur in Nature: meteorological, geochemical and pedological implications. Part II. *Tellus 12*, 63–109.

Ford, E. D. 1976. The canopy of a Scots pine forest: description of surface of complex roughness. *Agric. Meteorol. 17*, 9–32.

Goudriaan, J. 1977. *Crop micrometeorology:* a simulation study. Pudoc, Wageningen, 94–123.

Gravenhorst, G. and Höfken, K. D. 1982. Concentration of aerosol constituents above and beneath a beech and a spruce forest canopy. In *Deposition of atmospheric pollutants* (ed. H.-W. Georgii and J. Pankrath). D. Reidel Publishing Company, 187–190.

Hicks, B. B. 1980. On the dry deposition of acid particles to natural surfaces. In *Polluted rain* (ed. T. Y. Toriba, M. W. Miller and P. E. Morrow). Plenum Publ. Co., 327–339.

Holmes, M. G. and McCartney, H. A. 1976. Spectral energy distribution in the natural environment and its implications for phytochrome function. In *Light and plant development* (ed. H. Smith). Butterworths, London, 467–476.

Hosker, R. P. and Lindberg, S. E. 1982. Review: Atmospheric deposition and plant assimilation of gases and particles. *Atmos. Environ. 16*, 889–910.

Husar, R. B. 1974. Recent developments in *in situ* size spectrum measurement of submicron aerosols. In *Instrumentation for monitoring air quality*, ASTM STP 555, American Society for Testing and Materials, 157–192.

Jarvis, P. G., James, G. B. and Landsberg, J. J. 1976. 7. Coniferous forests. In *Vegetation and the atmosphere, Vol. 2* (ed. J. L. Monteith). Academic Press, London, 171–240.

Lannefors, H., Hansson, H.-C. and Granat, L. 1983. Background aerosol composition in southern Sweden—fourteen micro and macro constituents measured in seven particle size intervals at one site during one year. *Atmos. Environ. 17*, 87–101.

Little, P. and Wiffen, R. D. 1977. Emission and deposition of petrol engine exhaust Pb—I. Deposition of exhaust Pb to plant and soil surfaces. *Atmos. Environ. 11*, 437–447.

Liu, B. Y. H., Oiu, D. Y. H. and Rubow, K. L. 1983. Characteristics of air sampling filter media. In *Aerosols in the mining and industrial work environments, vol. 3* (ed. V. A. Marple and B. Y. H. Liu). Ann Arbor Science, London, 889–1038.

Malqvist, K. G., Johansson, G. I. and Akselsson, K. R. 1982. A facility for multielemental analysis by PIXE and the $^{19}F(p, \alpha\gamma)^{16}O$ reaction. *J. Radioanalyt. Chem. 74*, 125–147.

Marple, V. A. and Willeke, K. 1976. Inertial impactors: theory, design and use. In *Fine particles* (ed. B. Y. H. Liu). Academic Press, London, 411–446.

Massman, W. J. 1982. Foliage distribution in old-growth coniferous tree canopies. *Can. J. For. Res. 12*, 10–17.

Monteith, J. L. 1973. *Principles of environmental physics.* Arnold, London, 78–99.

Monteith, J. L. 1976. Spectral distribution of light in leaves and foliage. In *Light and plant development* (ed. H. Smith). Butterworths, London, 447–460.

Munn, R. E. 1966. *Descriptive micrometeorology*. Academic press, New York, p. 83.

Perrier, A. 1976. Study and attempt to model mass and energy exchanges in vegetation canopies. (In French.) Ph. D. Thesis, University of Paris VI Avril 1976, Paris, 99–114.

Rauner, L. J. 1976. Deciduous forests. In *Vegetation and the atmosphere, vol. 2* (ed. J. L. Monteith). Academic Press, London, 241–264.

Ross, J. 1975. Radiative transfer in plant communities. In *Vegetation and the atmosphere, vol. 1* (ed. J. L. Monteith). Academic Press, London, 13–55.

Spurny, K. R. and Lodge, J. P. 1972. Collection efficiency tables for membrane filters used in the sampling and analysis of aerosols and hydrosols. NCAR-TN/STR-77, NCAR, P.O. Box 3000, Boulder, Colorado, 80307.

Swank, W. T. and Schreuder, H. T. 1974. Comparison of three methods of estimating surface area and biomass for a forest of young eastern white pine. *Forest Sci. 20*, 91–100.

Thom, A. S. 1975. Momentum, mass and heat exchange of plant communities. In *Vegetation and the atmosphere, vol. 1* (ed. J. L. Monteith). Academic Press, London, 57–109.

Ulrich, B. and Pankrath, I. (Eds.) 1983. *Effects of accumulation of air pollutants in forest ecosystems*. D. Reidel Publ. Co., Dordrecht.

Whitby, K. T. 1978. The physical characteristics of sulfur aerosols. *Atmos. Environ. 12*, 135–159.

Wiman, B. L. B. 1981. Aerosol collection by Scots pine seedlings: design and application of a wind tunnel method. *Oikos 36*, 83–92.

Wiman, B. L. B. and Ågren, G. I. 1985. Aerosol depletion and deposition in forests—a model analysis. *Atmos. Environ. 19*, 335–347.

Wiman, B. L. B. and Lannefors, H. O. 1985. Aerosol characteristics in a mature coniferous forest—methodology, composition, sources and spatial concentration variations. *Atmos. Environ. 19*, 349–362.

Wiman, B. L. B., Ågren, G. I. and Lannefors, H. O. 1985. Aerosol concentration profiles in a mature coniferous forest—model versus field data. *Atmos. Environ. 19*, 363–367.

Yeh, G.-T. and Brutsaert, W. 1971. Sensitivity of the solution for heat flux or evaporation to off-diagonal turbulent diffusivities. *Water Resour. Res. 7*, 734–735.